공학석사 학위논문

Aerodynamic drag force on bridge deck in a large-scale along-wind velocity fluctuation

기류방향 장파장 변동풍속이 교량데크 항력에 미치는 영향

2017 년 2 월

서울대학교 대학원

건설환경공학부

백 승 열

ABSTRACT

This paper sets two main objectives which are the generation of large-scale along-wind velocity fluctuation and the evaluation of the aerodynamic admittance function for the 2nd Jin-do bridge for comparison with the Davenport function.

For the first objective, to generate large-scale along-wind velocity fluctuation, it is important to set the appropriate target wind properties. These properties are commonly determined by field instrumentation data or the target of the experiment. Using the active turbulence generator, it is experimentally verified that the relationship between the angle of the wing plate and the amplitude of the along-wind velocity fluctuation is linear. At the first trial, measured wind velocity fluctuation is not similar with the target spectrum density. Therefore, to match the generated wind to the target, trial and error method is selected to compensate the shortage.

As for the second objective which is the evaluation of the aerodynamic admittance function for 2nd Jin-do bridge and comparing it with the Davenport function, the aerodynamic admittance function value of the 2nd Jin-do bridge is around 50~60% of Davenport value for a 10% turbulence intensity and a large-scale turbulence length experiment.

Keyword: Aerodynamic, Large-scale, wind velocity fluctuation, active turbulence generator, admittance function.

Student Number: 2014-22704

TABLE OF CONTENTS

LIST OF FIGURES

LIST OF TABLES

CHAPTER 1

INTRODUCTION

In its natural condition, wind velocity is generally fluctuating and most of the time wind is not a smooth flow. Wind contains three kinds of velocity fluctuation components which are the longitudinal, lateral and vertical components. When a structure such as a bridge is subject to wind, wind actually acts on the structure as a load. Previous studies define the relationship between the wind velocity fluctuation and force response as an aerodynamic admittance function. Davenport (1962) proposed the longitudinal direction aerodynamic admittance function (AAF) in terms of frequency based function. Sears (1941) as well proposed the vertical direction AAF.

In case of the longitudinal direction AAF, Davenport function has been generally used for aerodynamic analysis. In the wind tunnel test, however, it is verified that measured AAF has a quite different value from the analytic value. Kazutoshi et al, (1999) paper points out that the correlation of drag force and the wind velocity fluctuation has a different value each other in contrast with the assumption of Davenport. In this paper, however, generated wind velocity fluctuation did not reflect the natural wind characteristics in terms of turbulence length scale. Only turbulence intensity is considered as an important parameter.

In addition, although it is not drag force part, Kawatani and Kim (1992) also measured the lift force AAF which comes from the along-wind velocity fluctuation.

For Davenport function, AAF value starts from the unit value and decreases slowly as wind frequency increases. However, in this study, there is a part which has values greater than one. Many studies indicate a problem in the AAF values: unlike Davenport function, the part greater than one is often found in the experiment.

Therefore, there are two research objectives in this paper. The first objective is the generation of large-scale along-wind velocity fluctuation using the Active Turbulence Generator (ATG), and the second objective is the evaluation of AAF for 2nd jin-do bridge to compare it with the Davenport function.

CHAPTER 2

Experiment Set Up

2.1 Active Turbulence Generator (ATG)

The active turbulence generator consists of wings linked in pairs. The bottom wing moves down when the upper wing moves up and moves up when the upper one moves down. The ATG is composed of several wing pairs.

Figure 1 shows the ATG when stopped. The angle of the wing and the exciting frequency is determined by the input voltage value. The maximum input voltage is 10V and the maximum exciting frequency is 10Hz. Time interval of input voltage is 0.01s. This system controls the longitudinal wind velocity fluctuation disturbing the wind flows.

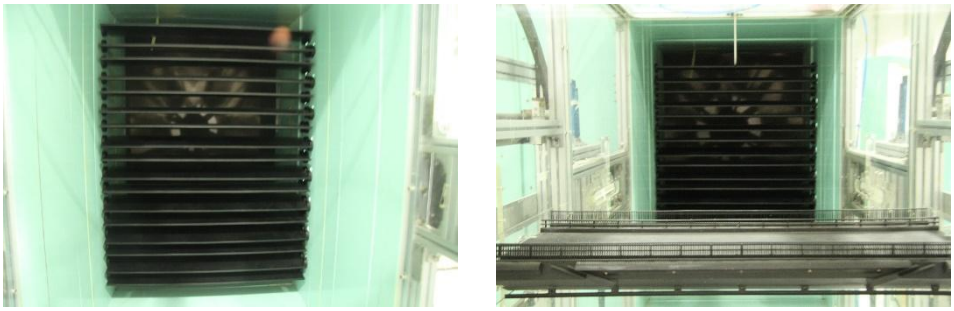

Figure 1. Active Turbulence Generator

2.2 Bridge section model

The model used for experiment is a 1:36 scale 2nd Jin-do bridge section model. Figure 2 shows the bridge model section. The wind velocity fluctuation component and force response is measured at 1.8m from the ATG. Force response is measured by 3-axial load cell positioned at the same distance from the ATG. Figure 3 shows the detailed figure of the wind tunnel measuring the raw data.

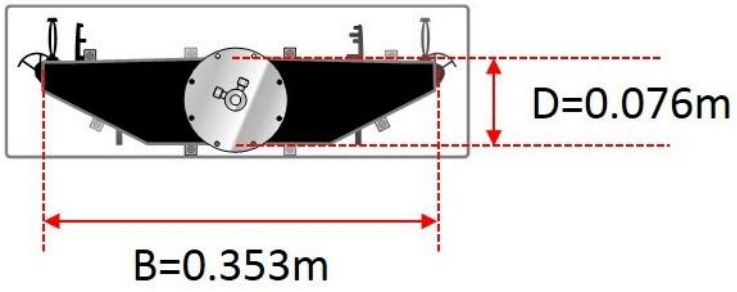

Figure 2. The bridge section model (2nd Jin-do bridge)

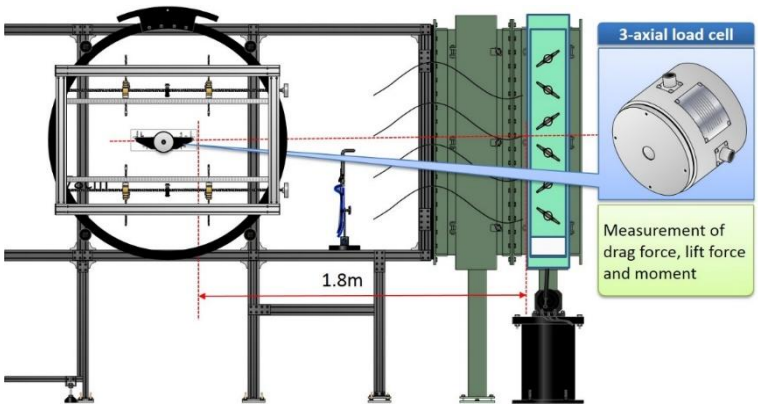

Figure 3. Detailed figure of the wind tunnel when ATG installed

CHAPTER 3

Generation of target large-scale along-wind velocity fluctuation

3.1 Simulation of wind velocity fluctuation

Von-Karman(1948) proposed a natural wind property in the shape of the auto spectrum density. For the the along-wind velocity fluctuation, it is written as:

$$\frac{f \cdot S_u(f)}{\sigma_u^2} = \frac{4 \cdot f \cdot L_u / U}{\left(1 + 70.8 \cdot \left(f \cdot L_u / U\right)^2\right)^{5/6}}$$

, where f =frequency(Hz), σ_u =standard deviation of along-wind velocity fluctuation, L_u =turbulence length scale of along-wind velocity fluctuation, U =mean wind velocity, S_u =Auto spectrum density of along-wind velocity fluctuation. Using this formulation, time signal of target wind can be obtainable. First, suppose that wind velocity fluctuation is a sum of harmonic component.

$$u(t) = \lim_{N \to \infty} \sum_{k=1}^{N} c_k \cdot \cos\left(\omega_k t + \varphi_k\right)$$

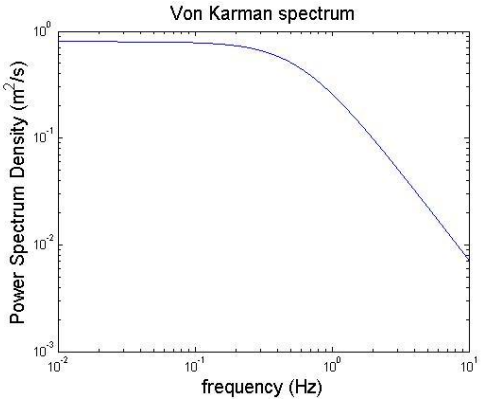

Figure 4. Von-Karman Spectrum

, where u =along-wind velocity fluctuation component, c_k =amplitude, φ_k =phase angle, ω_k =angular frequency(Hz). And second, according to the definition of the single-sided auto spectrum density, amplitude (c_k) is expressed as follows:

$$S_u(\omega_k) = \frac{E\left[\left(c_k \cdot \cos(\omega_k t + \varphi_k)\right)^2\right]}{\Delta\omega}$$

$$= \lim_{N\to\infty} \frac{1}{\Delta\omega} \cdot \frac{1}{T} \int_0^T \left[c_k \cdot \cos(\omega_k t + \varphi_k)\right]^2 dt = \frac{c_k^2}{2\Delta\omega}$$

$$\therefore c_k = \sqrt{2 \cdot \Delta\omega \cdot S_u(\omega_k)} = \sqrt{2 \cdot \Delta f \cdot S_u(f_k)}$$

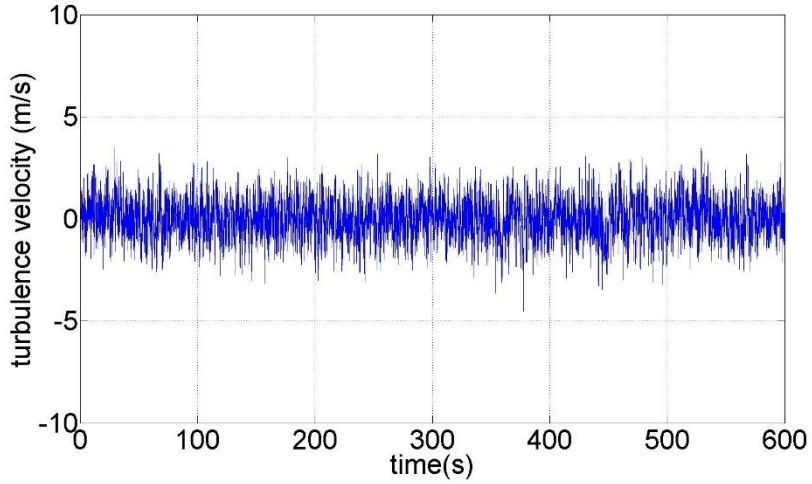

Figure 5. Time signal of simulation wind

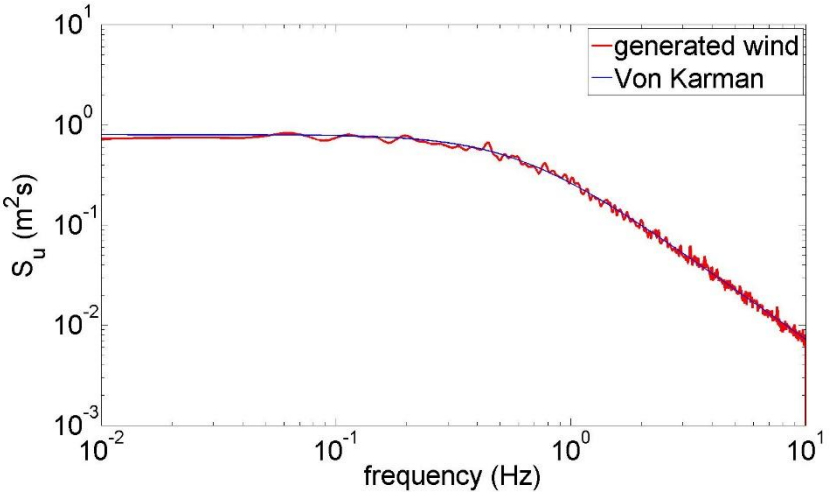

Figure 6. Comparison between Von-Karman Spectrum and simulation wind spectrum

After the determination of the frequency range what we want to see and the random phase, the amplitude of each sinusoidal wave is determined by target Von-Karman spectrum. Afterwards, time signal of target wind velocity fluctuation is determined as seen in Figure 5. The auto Spectrum density of the simulated wind is well-fitted to the Von-Karman Spectrum in Figure 6.

3.2 Conversion of time signal to Active Turbulence Generator(ATG) input value

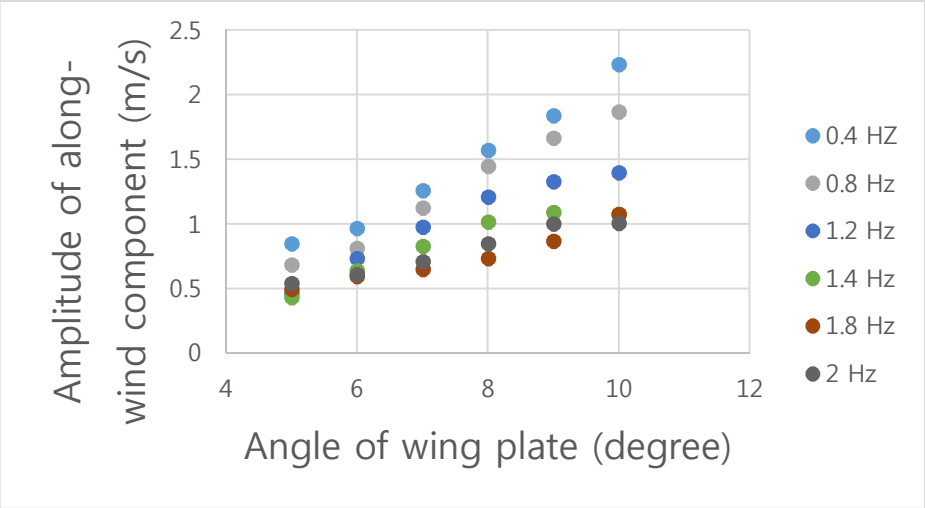

Figure 7. The relationship between amplitude of along-wind velocity fluctuation and angle of wing plate

By changing the motion angle and exciting frequency, the relationship between amplitude of along-wind velocity fluctuation and motion of ATG wing plate is verified through the experiment. Figure 7 shows that amplitude of along-wind component and angle of wing plate have a linear relationship. As for formula type, this relationship is written as:

$$\frac{|u|}{U} = 0.182|\theta|$$

, where $|u|$=amplitude of along-wind velocity fluctuation, $|\theta|$=angle of the moving wing plate. The constant value 0.182 is determined by an experiment. As the location of measurement hot-wire anemometer changes, this value will also change to another constant value. In case of exciting frequency, it is hard to find clear relationship with along-wind velocity fluctuation.

3.3 Generation of the target wind by trial and error method using ATG

ATG motor input values are generated from the simulation wind. Using this motor input data, large-scale along-wind fluctuation is produced by ATG. As shown in Figure 8 (a), the first trial is not well-fitted to the target Von-Karman spectrum. To compensate this shortage, trial and error method is used.

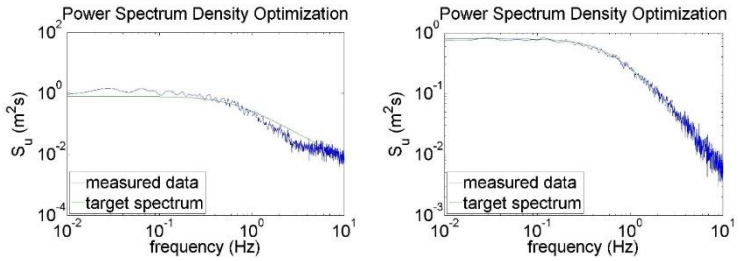

(a) (b)

Figure 8. Power spectrum density optimization to Von-Karman spectrum:

(a) first trial, (b) 3rd trial

After several trials for the trial and error approach, wind data generated by ATG is well-fitted to the target spectrum as depicted in Figure 8 (b). For Kim (2013) studies, the relationship between amplitude of along-wind velocity fluctuation and angle of wing plate is not considered as a factor of input data. Thus, to produce a well-fitted wind data, many steps of trial is needed to match the target spectrum density (over 10 times).

CHAPTER 4

Characteristics of measured wind velocity fluctuation

4.1 Comparison between generated wind and target wind

In general, target wind properties are determined by field instrumentation data. In the wind tunnel test, however, the dimensional parameter analysis needs to be considered. In this experiment, the following properties were used for the parameter analysis: 10m/s mean wind velocity, 10% turbulence intensity and 2m turbulence length scale**.**

Table 1. Comparison of measured wind the target wind

	Target property	Measured property	Error
Mean wind velocity(m/s)	10	9.886	1.1
Turbulence intensity(%)	10	9.860	1.4
Turbulence length scale(m)	2	1.888	5.6

Table 1 shows that properties of measured wind velocity fluctuation are close to the target properties with a 6% error. Other cases are also made with 10% error margin in my experiments. In case of turbulence length scale, there are two estimation methods to calculate this length scale. The first method uses auto

covariance coefficient, and the second one uses a curve fitting method through the Von-Karman spectrum. In our experiment. Turbulence length scale is calculated by curve fitting method.

4.2 Time signal comparison

In figure 8 (b) below, the auto spectrum density of measured wind velocity fluctuation is close to target von-Karman spectrum. In addition to frequency domain similarity, a time domain comparison is needed between the measured and the target wind.. Figure 9 shows that measured wind data has a similar trend with the target wind.

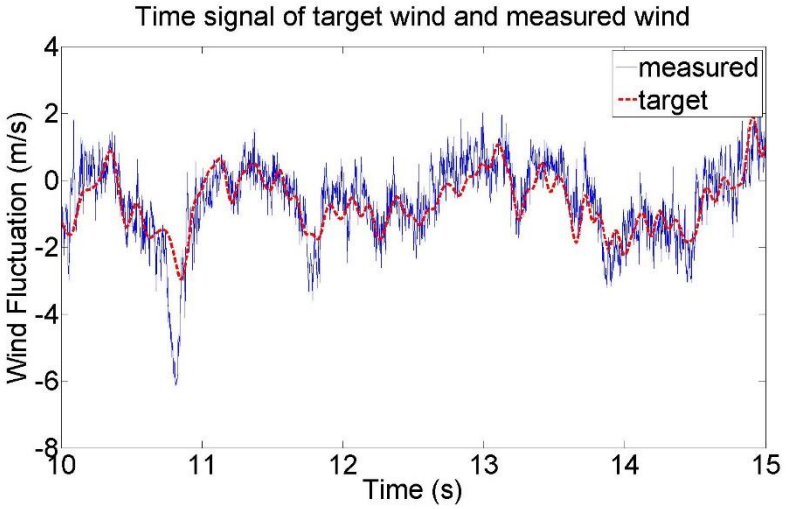

Figure 9. Time signal comparison of target wind fluctuation with measured wind fluctuation

The figure 9 shows, however, that measured wind fluctuation has two different characteristics compared with the target wind fluctuation. The first one is a sharply decreasing part between 10s and 11s. This part is found in entire time domain, and the size of this part is much bigger than target. This problem has to be solved by equipment improvement or other technical methods. The second one is the high

frequency noise. It is verified that this high frequency noises are caused from ATG wing plate and its motion and so, through the data filtering, the effect of the high frequency noises is cleared. Figure 10 shows the filtered wind data. Compare to original measured data. This filtered data is more similar to target wind fluctuation. In case mechanical filtering equipment like honeycomb is installed to decrease high frequency noises, more accurate and clear wind velocity fluctuation can be obtained.

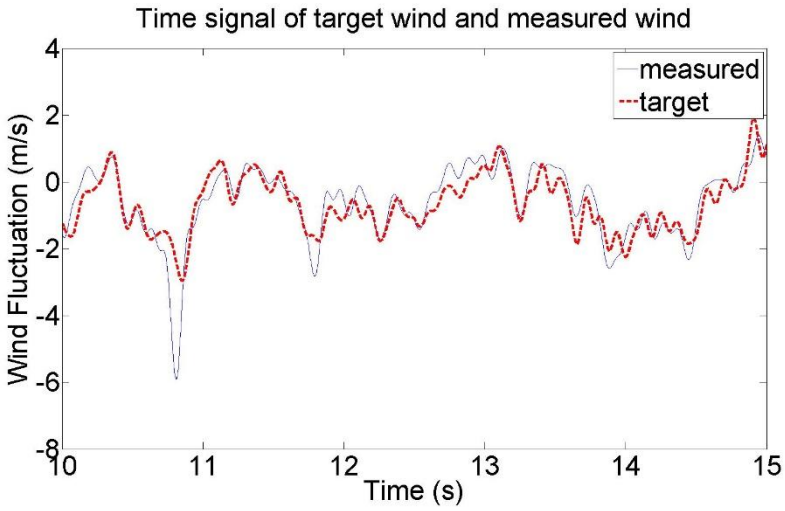

Figure 10. Measured wind fluctuation filtered by 10Hz

CHAPTER 5

Aerodynamic Admittance Function (AAF)

5.1 Formulation for longitudinal direction AAF

Drag force of wind velocity fluctuation at the bridge section is written as:

$$D_{buffet}(x,t) = \frac{\rho U^2 BL}{2}\left[2(D/B)\chi_{Du}C_D\frac{u}{D} + \chi_{Dw}\left(C_D^{'} - C_L\right)\frac{w}{U}\right]$$

, where , = static coefficient of drag and lift force respectively, = derivative of drag force static coefficient, =aerodynamic admittance function, , = along-wind and vertical wind velocity fluctuation component respectively. The auto spectrum density is obtained through the analysis in frequency domain both sides. It is written as:

In the case of the 2nd Jin-do bridge, along-wind velocity fluctuation part is times higher than vertical wind velocity fluctuation part. Therefore, the auto spectrum density of drag force can be written as:

$$S_D(f) = \left(\frac{\rho UBL}{2}\right)^2\left[\left(2(D/B)C_D\right)^2|\chi_{Du}|^2 S_u(f) + \left(C_D^{'} - C_L\right)^2|\chi_{Dw}|^2 S_w(f)\right]$$

Amplitude of aerodynamic admittance function is calculated by the following formulation.

$$|\chi_{Du}|^2 = \frac{S_D(f)}{(\rho UDLC_D)^2 S_u(f)}$$

5.2 Evaluation of Aerodynamic Admittance Function

Figure 11 shows that the AAF of 2nd Jin-do bridge is 50~60% the Davenport value. This means that there may be a load reduction effect compared with the quasi-static theory in the aerodynamics. To identify this load reduction effect,

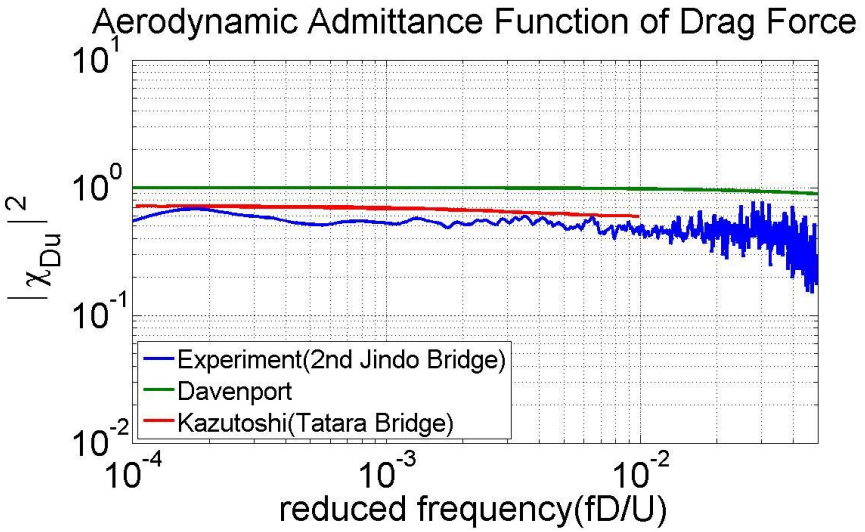

Figure 11. Aerodynamic admittance function of drag force

simultaneous force measurement experiment is needed to obtain spatial correlation at various points along with the lateral direction of the bridge. Unlike the assumption of Davenport stating that bridge width is almost equal to its depth, the bridges built nowadays have a streamlined shape to prevent aerodynamic instability. Consequently, the exact evaluation of the longitudinal direction aerodynamic admittance function will be crucial for a better understanding of bridges' behavior.

Conclusion

Through the relationship between the amplitude of the along-wind velocity fluctuation and the motion angle of wing plate, a large-scale along-wind velocity fluctuation was generated in the wind tunnel using the Active Turbulence Generator. The generated wind velocity parameters such as the turbulence intensity and length scale were found to be within 6% from the target wind parameters. As for time domain analysis, two main points deserve to be mentioned. The first point is a sharply decreasing part of the curve. This decreasing part is shown in the entire time domain. When the simulation of the wind velocity fluctuation decreases in the input data, a sharply decreasing phenomenon actually happens in the experiment. Furthermore, the size of this part is at least 2~3times bigger than the target wind. To get a more accurate wind values compared to the target, this problem would have to be fixed by improved equipment or other methods. The second main point to be underlined is a high frequency noise. This noise may be generated by the installed ATG wings and its movement. It was verified that this concern can be overlooked if a more accurate wind data is obtained by a frequency filtering equipment like a honeycomb.

In addition to generating the target wind velocity fluctuation, Aerodynamic Admittance Function(AAF) of 2nd Jin-do bridge is also calculated for the drag force of the bridge using a three axial load cell. AAF value of 2nd jin-do bridge has a value of 50~60% Davenport proposed one. This leads to a conclusion that a load recution

effect in the aerodynamic analysis needs to be considered. Even though Davenport proposed the AAF equation in terms of drag force, this result shows that the AAF value needs to be experimentally checked.

Reference

Sears, W. R. (1941) “Some aspects of non-stationary airfoil theory and its practical application.” J. Aeronautics Sci, 8(3), 104-108

Davemport (1962) “Buffeting of a suspension bridge by storm winds”, *Journal of STRUCTURAL DIVISION.* ASCE vol. 88 (ST3) (1962) 233-268.

Strommen, E. N. (2010) “Theory of Bridge Aerodynamics”, Springer, pp.91-108.

M. Kazutoshi., H. Yuichi., F. Tohru., M. Akira. (1999) "Aerodynamic admittance and the ‘strip theory’ for horizontal buffeting force on a bridge deck”, *Journal of Wind Engineering and Industrial Aerodynamics 83 (1999) 337-346*

M. Kawatani., and H. Kim. (1992) “Evaluation of Aerodynamic Admittance for Buffeting Analysis”, *Journal of Wind Engineering and Industrial Aerodynamics 41-44 (1992) 613-624*

Diana, G., Bruni, S., Cigada, A. and Zappa, E. (2002) “Complex aerodynamic admittance function role in buffeting response of a bridge deck,” Journal of Wind Engineering and Industrial Aerodynamics 90, 2057-2072

A. Wilson (2009) “A Critical Analysis of Tatara Bridge, Japan”, University of Bath.

Scanlan, R. H. and Jones, N. P. (1999) “A form of aerodynamic admittance for use in bridge aeroelastic analysis,” J. Fluids and Structure. 13, 1017-1027

Hatanaka. A., Tanaka. H., (2002) “New estimation method of aerodynamic admittance function”, Journal of Wind Engineering and Industrial Aerodynamics 90, 2073-2086.

Kim, S. W. (2013) “Evaluation of Frequency-dependent Aerodynamic Admittance Function in a Time Domain Buffeting Analysis,” Master dissertation, Seoul National University.

국 문 초 록

본 연구에서는 2가지 목표를 설정하고 실험을 수행하였다. 첫 번째 목표는 장파장 길이방향 변동풍속의 생성이고 두 번째 목표는 Davenport 가 제안한 함수값과 비교하여 제 2진도대교의 어드미턴스 함수를 구하는 것이다.

첫 번째 목표인 길이방향 장파장 변동풍속을 생성하기 위해서는 적절하게 바람의 특성값을 결정하는 것이 중요하다. 이러한 특성값은 보통 현장조사에 의해서 결정되거나, 실험의 목적에 의해서 결정된다. 능동난류 발생장치를 제어하면서, 길이방향 변동풍속의 크기와 능동난류방생장치 날개의 각도의 관계를 실험적으로 선형관계임을 파악하였다. 그러나 첫번째 시도에서는 목표 스펙트럼과 차이를 가지는 변동풍속을 가지게 되고, 이러한 오류를 줄이기 위해서 여러 번의 시행착오법을 사용하였다.

두 번째 목표로써 제 2 진도대교의 어드미턴스 함수를 Davenport 가 제안한 함수값과 비교해보면, 제 2 진도대교의 어드미턴스 함수는 Davenport 의 값에 비해서 50~60% 정도의 값을 가지는 것으로 확인되었다.

주요어: 공기동역학, 장파장, 변동풍속, 능동난류발생장치, 어드미턴스 함수

학번: 2014-22704